
The Over-Certainty Phenomenon in Modern UDA Algorithms

Fin Amin

North Carolina State University

Jung-Eun Kim*

North Carolina State University

Abstract

When neural networks are confronted with unfamiliar data that deviate from their training set, this signifies a domain shift. While these networks output predictions on their inputs, they typically fail to account for their level of familiarity with these novel observations. While prevailing works navigate unsupervised domain adaptation with the goal of curtailing model entropy, they unintentionally birth models that grapple with sub-optimal calibration - a dilemma we term the over-certainty phenomenon. In this paper, we uncover a concerning trend in unsupervised domain adaptation and propose a solution that not only maintains accuracy but also addresses calibration.

1 Introduction

When encountering new environments, humans naturally adopt a cautious approach, assimilating the novelty to guide their decision-making. This inherent ability to assess unfamiliarity and adjust certainty has not been entirely emulated in artificial neural networks. Unlike humans who might exhibit hesitation in unknown situations, many unsupervised domain adaptation (UDA) algorithms lack an explicit mechanism to modulate certainty in response to the novelty or unfamiliarity of their inputs.

Deep learning has never been a stranger to the challenges of uncertainty. Over the past few years, the miscalibration problem of modern neural networks has gained substantial attention, as highlighted by works such as [1], [2], [3], and [4]. However, there is an observed void in the landscape of unsupervised domain adaptation techniques, with most of them neglecting model calibration during the adaptation processes. In this paper, we introduce the *over-certainty phenomenon* which harms model calibration, and propose an algorithm that extends the notion of unfamiliarity - analogous to what humans experience - to UDA.

A prevailing strategy among UDA algorithms is the minimization of entropy, either as an explicit target or as an inherent by-product of their methodology. And while this might bolster accuracy metrics, our research indicates a concerning trend: excessive entropy reduction can be detrimental to model calibration. What makes this trend more problematic is that it occurs within the context of a new domain, where epistemic uncertainty should typically be greater. **In our work, we**

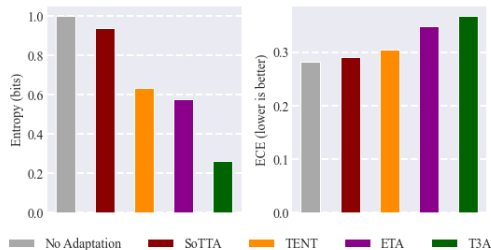


Figure 1: This chart shows four modern UDA algorithms adapting EfficientNet to the *clipart* domain. Minimizing entropy is a common objective in recent work. However, this can have consequences on model calibration.

*Correspondence

measure certainty as the inverse of Shannon entropy of a model’s output after a softmax operation: $H(f(x))^{-1} = (\text{Entropy}_2(\text{SM}(f(x))))^{-1}$.

To further frame our discussion, UDA is used when a model, trained on a source domain (X_s, Y_s) , is presented with the challenges of a different yet analogous target domain (X_t) with no labels.

In our problem setting, we do not assume access to X_t until we adapt. The nuances between these domains, commonly termed as domain shift, can introduce significant disruptions in model performance. UDA, in its essence, aspires to adapt the insights harvested from the source domain and apply them proficiently to the target domain, bypassing the need for labeled data in the latter. Thus, within the context of this domain shift, it can be especially problematic to be too certain [5].

With the purpose of addressing these intertwined challenges, we introduce *Dynamic Entropy Control*. This UDA technique seeks to augment accuracy, improve model calibration, and have low computational overhead. By interweaving calibration into the core learning process, we produce a UDA adjustment algorithm that jointly improves accuracy while managing epistemic uncertainty. To summarize, our contributions are:

- The identification of the over-certainty phenomenon in modern UDA algorithms. **We emphasize that our work is *not* about the well-studied incidence of how models become less calibrated when used in new domains** [4, 6]. It is, however, about showing how **UDA algorithms** engender poorly calibrated models - sometimes **beyond** baseline. To the best of our knowledge, there are no existing works which identify this. We provide thorough empirical evidence which corroborates our claims. Furthermore, we provide plausible explanations as to why this happens. In our work, we focus on the classification setting.
- *Dynamic Entropy Control*, a new UDA algorithm that achieves SOTA calibration in all of the four datasets and SOTA accuracy uplifts in the majority of domain shifts. Additionally, our algorithm provides favorable memory consumption vs. performance trade-offs.

2 Related Work and State-Of-The-Arts

We divide our literature survey into two sections. The first section covers methodologies catered towards updating a neural network on unlabeled data. For the sake of brevity, we will refer to unlabeled data as “observations.” This section gives an overview of the work done to improve networks on the fly. We start by introducing earlier work, such as dictionary learning techniques, and lead our way into recent developments. The second section covers how calibration is measured and improved in the context of a domain shift. Furthermore, we provide a supplementary discussion of related work in the appendix.

2.1 Self-Taught Learning and UDA

The phrase “self-taught learning” was coined by [7]. In this work, the authors utilize observations to find an optimal sparse representation of said observations. This sparse representation is used to train their model in lieu of the ordinary training set to improve out-of-distribution (OOD) performance.

Work in this field has extended to a variety of approaches such as the use of pseudo-labeling to exploit the existing model’s predictions as target labels [8, 9, 10]. Pseudolabeling can be thought of under the guise of knowledge distillation (KD) [11, 12]. KD is a transfer learning paradigm where a large neural network, known as the teacher, transfers “knowledge” to a smaller “student” network. Succinctly, the student is trained to match the output of the teacher when given the same input as the teacher [13]. In pseudo-labeling, the teacher and student are the same network.

More recent advancements include TENT [14], EATA/ETA [15], T3A [16] and SoTTA [17]. The TENT algorithm introduces the trend of **test-time entropy minimization**. Entropy minimization can be thought of as using pseudo labels with the cross entropy loss function. In other words, the entropy minimization works by using gradient descent to minimize:

$$L_{TENT} = - \sum_{y \in C} f(y|x) \log f(y|x) \tag{1}$$

Algorithm	Tier 1	Tier 2	Tier 3	Tier 4	Tier 5	Algorithm	Tier 1	Tier 2	Tier 3	Tier 4	Tier 5
No Adapt	2.00 _{0.17}	2.10 _{0.22}	2.25 _{0.30}	2.44 _{0.51}	2.63 _{0.73}	No Adapt	0.23 _{0.02}	0.26 _{0.03}	0.29 _{0.03}	0.32 _{0.04}	0.34 _{0.04}
DEC (ours)	4.48 _{0.25}	4.68 _{0.34}	4.90 _{0.53}	5.01 _{0.77}	5.32 _{0.80}	DEC (ours)	0.08 _{0.01}	0.08 _{0.02}	0.07 _{0.02}	0.06 _{0.02}	0.04 _{0.03}
T3A	1.36 _{0.11}	1.41 _{0.14}	1.46 _{0.17}	1.60 _{0.20}	1.74 _{0.23}	T3A	0.33 _{0.03}	0.35 _{0.03}	0.38 _{0.03}	0.41 _{0.04}	0.43 _{0.04}
ETA	1.37 _{0.08}	1.47 _{0.14}	1.57 _{0.23}	1.71 _{0.38}	1.87 _{0.67}	ETA	0.37 _{0.03}	0.40 _{0.03}	0.41 _{0.04}	0.43 _{0.04}	0.44 _{0.04}
TENT	1.40 _{0.08}	1.48 _{0.12}	1.57 _{0.19}	1.62 _{0.33}	1.79 _{0.49}	TENT	0.27 _{0.02}	0.30 _{0.03}	0.33 _{0.03}	0.36 _{0.04}	0.39 _{0.04}
SoTTA	1.71 _{0.07}	1.78 _{0.12}	1.88 _{0.18}	2.08 _{0.31}	2.26 _{0.41}	SoTTA	0.20 _{0.02}	0.21 _{0.02}	0.23 _{0.03}	0.25 _{0.03}	0.28 _{0.03}

(a) Average Shannon Entropy over Domain Shifts

(b) Average ECE (lower is better) over Domain Shifts

Table 1: Comparison of entropy and ECE averaged across the 15 domain shifts of TIN-C. We use the EfficientNet _{$\beta=98\%$} backbone. Standard deviations across the domains are shown as subscripts. This experiment shows the relationship between *calibration* and *certainty* (the inverse of entropy). Existing UDA algorithms achieve sub-optimal calibration due to excessive certainty on their predictions. **Our reduction in ECE is statistically significant with $p < 0.01$.** Note that we also achieve very competitive accuracy (see Table 4).

to update the model’s batch-normalization parameters. ETA² advances on TENT by making sure that observations are *reliable* and *non-redundant* before they are used for updating the batch-normalization parameters. To do this, they compute a sample adaptive weight, $\mathcal{S}(x)$, for each observation before minimizing entropy:

$$L_{ETA} = -\mathcal{S}(x) \sum_{y \in \mathcal{C}} f(y|x) \log f(y|x) \quad (2)$$

where $\mathcal{S}(x)$ is a function of the entropy of the model towards the batch sample (i.e., the reliability) and the similarity to what it has seen before (i.e., non-redundancy). Similar to the aforementioned methods, SoTTA minimizes entropy via sharpness-aware-minimization (SAM) [18]. The algorithm employs high-confidence uniform sampling to create a memory bank of size N_{SoTTA} which stores reliable and class-balanced observations. This is done by using confidence to assess if an observation should be used for adaptation. Confidence is defined as:

$$\mathcal{C}_f(x) = \max_{i=1, \dots, n} \frac{\exp(f(x)_i)}{\sum_{j=1}^n \exp(f(x)_j)} \quad (3)$$

If $\mathcal{C}_f(x) > \mathcal{C}_0$, where \mathcal{C}_0 is some pre-defined confidence threshold, then x is saved into memory. Afterwards, the SAM optimizer is used to minimize entropy (equation 1) via *two* backpropagation steps. The T3A algorithm [16] differs from the previous three as it focuses on updating the *prototypes* [19] of each class during test time:

$$S_k^t = \begin{cases} S_k^{t-1} \cup \{f(x)\}, & \text{if } \hat{y} = y_k \\ S_k^{t-1}, & \text{else.} \end{cases} \quad (4)$$

$$c_k = \frac{1}{|S_k^t|} \sum_{z \in S_k^t} z \quad (5)$$

where c_k represents the centroid of the prototypes of a class $k \in \mathcal{C}$, where \mathcal{C} is the number of classes. We define the feature extractor, ψ , as all the layers of the backbone before the final dense layer. The final dense layer, ϕ , is what we refer to as the classifier, it is composed of the class centroids. We denote the output of the feature extractor as $z = \psi(x)$. To inference, T3A computes:

$$\operatorname{argmax}_{y_k} \frac{\exp(z \cdot c_k)}{\sum_j \exp(z \cdot c_j)} \quad (6)$$

Unlike TENT, SoTTA or ETA, T3A does not use back propagation. However, similar to ETA, this algorithm filters less reliable samples during equation 4 by only keeping the M lowest entropy prototypes for each class. Therefore, the algorithm stores $C \cdot M$ prototypes.

2.2 Neural Network Calibration

Neural network calibration has been of intense interest in recent years due to the critical role of confidence values, which reflect the probability assigned to predictions, in various applications. For

²While the authors of EATA/ETA introduce two similar algorithms, for our paper, we focus on ETA.

instance, BranchyNet [20] uses neural network confidence to enable early exits for faster inference, relying on high confidence at intermediate layers. However, [21] highlights the prevalent issue of certainty calibration in deep networks, where models often display overconfidence or underconfidence, likely due to overfitting during training. The authors of [6] explore this concept further. They measure a model’s expected calibration error (ECE) with respect to changes (rotation, translation, etc) in the test set. ECE measures how closely the confidence levels of a model’s predictions match the actual probability of those predictions being correct. It calculates the average absolute difference between predicted confidence and the true outcome frequencies, providing a metric for the reliability of the model’s probabilistic outputs. **We follow their convention and use ECE as our measure for calibration error.** They notice models calibrated on the validation set tend to be well calibrated on the test set, but are not properly calibrated to shifted data. Recent work has also investigated solutions to this phenomenon. [1] discusses a technique known as temperature scaling while [22] approaches this problem by regularizing the logit norm. More classical solutions to this problem exist as well; [23] and [24] consider label smoothing to address this issue. Note that these techniques are addressed at calibrating the underlying backbone but have *not* been investigated with respect to UDA algorithms themselves.

There has been attention in recent years in the problem of determining if, and to what degree, an observation is similar to what a model was trained on. For example, the authors of [25] observe that if an autoencoder was trained to reconstruct inliers, it would have a greater reconstruction error when reconstructing OOD data. [26] and [27] approach this issue by observing that the discriminator of a GAN learns whether or not a given input is an inlier. Many other works delve into this domain [28, 29, 30, 31, 32, 33, 34]. Regarding the UDA algorithms we compare against, the most common proxy for reliability is entropy on the observation.

3 Proposed Approach

3.1 The Over-Certainty Phenomenon

In this work, we present evidence for what we dub the *over-certainty phenomenon* (OCP) of contemporary UDA approaches. This phenomenon is that UDA algorithms tend to miscalibrate their underlying backbone networks by causing their predictions to be excessively certain. Modern UDA algorithms often strive to decrease test-time entropy. However, as shown in Fig. 1, this entropy reduction may increase ECE because the models become overly certain on their predictions.

This phenomenon of existing algorithms causing models to become overly certain presents itself across many other datasets. A compelling example is given in Table 1 which agglomerates calibration errors over 15 domain shifts; in this table, we see a clear trend of entropy reduction (certainty increasing) and sub-optimal calibration. Another example is provided in Table 2a, T3A reduces entropy by a factor of about 4 in the *art*, *clipart* and *product* domains. As before, it causes ECE to worsen compared to the baseline. We do not claim that UDA algorithms should *always* strive to increase backbone uncertainty; poor calibration can also be caused by under-certainty and there exist cases where reducing entropy compared to baseline improves calibration. However, we find that the resulting calibration is still sub-optimal. Despite these complexities, our investigation reveals a consistent pattern: *the over-certainty phenomenon causes sub-optimal model calibration*, a significant concern for safety, robustness, and reliability.

3.2 What Causes the Over-Certainty Phenomenon?

We identify two plausible causes of the OCP, the first issue is that modern UDA algorithms aim at minimizing backbone entropy too aggressively. In the case of TENT, ETA, and SoTTA, their loss functions, equations (1) and (2), explicitly aim at reducing a model’s entropy. Regarding TENT, there is no regularization of this process. In the case of ETA, the algorithm uses a *reliability score*, $S(x)$, which aims at weighing observations differently but does not regularize the distributions of the pseudo-labels. Unlike the other two, SoTTA minimizes entropy twice per iteration. T3A does not explicitly reduce entropy as it does not use a loss function, but the authors claim this as an effect of using their algorithm. In fact, they show in certain datasets T3A reduces entropy more than TENT does.

Another issue is how existing methods evaluate observation *reliability*, the suitability of a model’s prediction for use for adaptation. Previous works, ETA and T3A, tap into the power of model certainty, using it to weigh the influence of observations. ETA assesses reliability by ensuring that observations meet a certain entropy threshold; similarly, T3A uses entropy to sort the importance of class prototypes. However, as prior work has shown, there are drawbacks in using entropy as a proxy for reliability in this manner [22]. To illustrate our point, we give a toy example of how using entropy can lead to a misleading conclusion:

Example 1 Suppose that we analyze the classifier while classifying between two classes with class centroids, c_0 and c_1 . This is done by taking the output of the feature extractor, $\psi(x) = z$, and computing the dot product between the centroids and z .

$$g = [z \cdot c_0, z \cdot c_1] \tag{7}$$

Consider g_{t1} , g_{t2} and g_s as vectors representing the inner products related to two observations, x_{t1} and x_{t2} , and to a specific training sample, x_s . Specifically, g corresponds to the dot products between the output of the feature extractor and the class centroids. As an example, let’s assume:

$$g_s = [8.0, 7.29]; \quad g_{t1} = [1.9199, 1.00019]; \quad g_{t2} = [6.1, 6.5];$$

If we take the softmax of these vectors and compute the entropy, we get $\text{Entropy}_2(\text{SM}(g))$ for g_s , g_{t1} and g_{t2} , as 0.92 bits, 0.86 bits and 0.97 bits, respectively.

Notice that if we consider the entropy of these three vectors as a proxy for reliability, we would consider x_{t1} to be more reliable than x_{t2} , despite x_{t2} having considerably greater average inner product with the class centroids. It is far more likely that the values of g_{t1} occurred due to spurious feature correlations between x_{t1} and the class centroids. In fact, in the scenario above, x_{t1} would be deemed to be more reliable than the genuine source domain observation x_s . Note that an analogous remark could be made on using confidence instead of entropy. Thus, in the example above, we would consider x_{t1} to be a confident sample. Note that our analysis is not contrived, as seen in Fig. 2. As we increase the domain shift intensity, the observation logit norm decays and has higher variance.

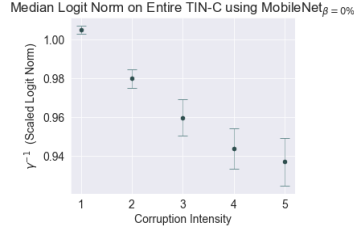


Figure 2: The median γ^{-1} value (step 8) from our CCR algorithm represents the ratio between the l_2 norms of the observation logits, z , and the training-set logits, κ . As z decreases, γ increases; this regularizes low-logit-norm observations more aggressively (step 9). Vertical bars indicate domain-to-domain standard deviations.

Furthermore, existing approaches do not consider a model’s certainty on the source domain. For example, ETA’s reliability paradigm rejects observations which have $H \geq 0.4 \cdot \ln(C)$. What if we *expect* (i.e. there was high entropy on the training set) the model to have high entropy? By only evaluating the target domain’s certainty without juxtaposing it against the source domain certainty, there is a lack of reference in terms of assessing the reliability of the observation. We address this issue via the h_0 parameter explained in the next section.

3.3 The Dynamic Entropy Control UDA Algorithm

To ameliorate the over-certainty phenomenon, we introduce Dynamic Entropy Control (DEC) (Algorithm 2). DEC refines the model’s certainty levels, aligning them more closely with its actual accuracy, by selectively adjusting the temperature parameter during the pseudo-labeling process (line 6). This is achieved without directly altering ground truth labels, instead focusing on the tempering of logits through temperature adjustments. **Our approach can be implemented using a single model which alternates weights. To facilitate understanding, we explain our algorithm as if it uses two distinct models:** the teacher and the student. The “teacher” model is simply f before any adaptation. The “student” model is simply a copy of f which we use to store the weight adaptations.

This process involves adjustments of the student model, guided by the comparative analysis of entropy and logit norms, thereby fostering a more accurate and reliable predictive model. The inputs f_{te} , f_s , h_0 , and X correspond with the teacher model, the student model, the teacher’s average

entropy on the training set, and unlabeled observations, respectively. The input κ is the median l_2 norm of the training-set logits; this gives us a context in terms of logit norms. The λ parameter is the learning rate for SGD, which we set to 0.001 for all experiments.

Algorithm 1 Compute Certainty Regularizer (CCR)

Input: $f_{te}(X), h_0, h_{max}, t_{min}, t_{max}, \kappa$
Output: T_{vec}

- 1: $Z = f_{te}(X)$ {get logits}
- 2: $H_{vec} = \text{Entropy}_2(\text{SM}(Z))$ {entropy for each sample}
- 3: $H_{diff} = H_{vec} - h_0$ {compare entropy with source entropy}
- 4: $H_{scaled} = \text{sigmoid}\left(\frac{H_{diff}}{\sqrt{h_{max}}}\right)$ {scale between [0,1]}
- 5: Initialize T_{vec} {compute regularizer for each observation:}
- 6: **for** $h_i \in H_{scaled}$ and $z_i \in Z$ **do**
- 7: $t_i = t_{min} + h_i \cdot (t_{max} - t_{min})$
- 8: $\gamma_i = \frac{\kappa}{\|z_i\|_2}$ {scale the logit norm}
- 9: $\tau_i = \gamma_i \cdot t_i$ {adjust regularizer via logit norm}
- 10: Store $T_{vec} \leftarrow \tau_i$
- 11: **end for**
- 12: **return** T_{vec}

DEC, we do not label smooth directly, but instead adjust the temperature parameter of our teacher during the adaptation process. To show how DEC regularizes observations appropriately, we continue from Example 1 to Example 2:

Example 2 Given the same g_{t1}, g_{t2} and g_s from Example 1, we input these into our CCR algorithm. We set $h_0 = H(\text{SM}(g_s)), \kappa = \|g_s\|_2, t_{min} = 1.0$ and $t_{max} = 2.0$. Our algorithm first computes a scaled entropy, H_{scaled} with respect to the source domain entropy for g_s, g_{t1} and g_{t2} , as 0.49, 0.48, and 0.50, respectively.

In step 7 of CCR, this entropy is transformed into a preliminary regularizer, t_i . Then, step 9 adjusts t_i by considering logit norm with respect to the source-domain logit norm.

$$\tau_{g_s} = 1.49; \quad \tau_{g_{t2}} = 7.42; \quad \tau_{g_{t1}} = 1.83$$

Notice that, unlike purely entropy-based methods, the CCR algorithm correctly assigns greater regularization to the less reliable samples. Namely, step 9 ensures that samples that are low-entropy due to degenerate reasons are properly regularized by considering logit norm. Furthermore, unique from existing algorithms, our regularizer directly addresses model certainty. The impact of CCR is analyzed in Fig. 3.

An interesting interpretation as to how our model improves accuracy is through the works of [35] and [36]. Although the former’s work concerns itself in the semi-supervised learning setting, we found their observations to be relevant. That is, they introduce the *noisy student*, a network that has been *noised* by dropout and stochastic-depth. They find that their noisy student can even learn to outperform the teacher

Compute Certainty Regularizer (Algorithm 1) returns a regularizer, $\tau_i \in T_{vec}$, for each observation, with respect to relative observation entropy and relative logit-norm. The parameter $h_0 = \mathbb{E}[H(\text{SM}(f_{te}(X_s)))]$ is used as a reference point; intuitively, the idea is to compare the model’s certainty on the observation with respect to the certainty of towards what it was trained on. Parameters t_{min} and t_{max} are used to shift the entropies into a valid range³. $h_{max} = \log_2(C)$ (maximum entropy is when all classes are equiprobable) is used to smoothen the sigmoidal function.

The τ parameter returned by Algorithm 1 plays a pivotal role. We name it the *certainty regularizer*. It regulates the “sharpness” of predicted probabilities and smoothen the pseudo labels produced by the teacher; as τ increases, the certainty on the prediction decreases. By preventing the model from becoming inappropriately certain in its predictions, we produce a model that is better calibrated — its prediction certainty more closely aligns with its true accuracy. In

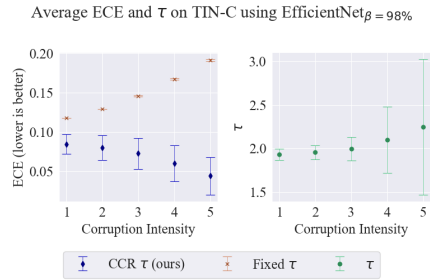


Figure 3: Our ablation study highlights the effectiveness of the CCR algorithm compared to a fixed τ optimized for minimal ECE on the source-domain training set. The rightmost figure displays the computed τ values, with vertical bars indicating domain-to-domain standard deviations.

³Because τ guides the temperature scaling component of our algorithm, we follow the convention of [1] and recommend setting $t_{min/max}$ within [1.0, 3.0].

Algorithm	Art	Clipart	Product	Real World
No Adaptation	0.9503	0.9507	0.7041	0.6889
DEC (ours)	2.2392	2.6147	2.0812	1.7949
T3A	0.1879	0.2309	0.1375	0.1705
ETA	0.9403	0.9658	0.7353	0.6782
TENT	0.9179	0.8949	0.6526	0.6365
SoTTA	0.9767	0.9710	0.7011	0.6849

(a) Shannon Entropy on Home Office.

Algorithm	Art	Clipart	Product	Real World
No Adaptation	0.3021	0.3155	0.1827	0.1694
DEC (ours)	0.0801	0.0466	0.0386	0.0179
T3A	0.4386	0.4177	0.2360	0.2484
ETA	0.3129	0.3238	0.2078	0.1719
TENT	0.2992	0.3083	0.1873	0.1718
SoTTA	0.2792	0.3008	0.1859	0.1672

(b) ECE on Home Office (lower is better).

Table 2: Our investigation reveals a pattern of existing UDA algorithms achieving sub-optimal calibration. We suspect this is caused by excessive entropy minimization. Experiment done using the MobileNet backbone on the Home Office dataset. Note that ECE values less than 0.01 are considered already well calibrated [1]. Our reduction in ECE is statistically significant with $p < 0.01$.

which initially produced the pseudo-labels. For the latter work, they establish that label smoothing mitigates label noise, which is a desirable property with respect to unsupervised adaptation. Specifically, they find that label smoothing can be thought of as a regularizer. **This motivates us to smooth more aggressively when we notice that an observation might be less reliable.**

To optimize memory efficiency, we freeze a large subset, β , of the weights of our student so that we only have to store the weights of the teacher network plus the weights which we choose not to freeze. The `Freeze_b_Layers(f_s, β)` function works by freezing the parameters of f_s . For notational purposes, we define β as the percentage of the backbone model that is frozen. We found empirically that freezing last (i.e., the layers closest to the output) b layers works the best – we surmise this is due to issues with embedding alignment as remarked by [37]. We select b so that β percent of our backbone model is frozen. Therefore the b value will vary across backbones for a target β value. In other words, to select b , one should compute the number of parameters in each layer and select b layers such that target percentage of network parameters, β is frozen.

4 Experiments

4.1 Experimental Setting

In order to evaluate DEC, we conduct a series of experiments using three different backbone models across four datasets. Our primary evaluation metrics will be model accuracy and $ECE_{bins=15}$ on the observations, allowing us to examine both the predictive performance and the calibration quality of the models. By using varied domains and different backbone architectures, we aim to demonstrate the robustness and adaptability of our algorithm in handling diverse and challenging unsupervised domain adaptation scenarios. All experiments are run three times. Note that the $t_{min/max}$ hyperparameters are set per dataset; we do not set these per domain shift. We use a `batchsize = 50` for DEC. The β parameter presented is only relevant to DEC. **We present accuracy and calibration for all datasets along with experiment variances either in the main paper or the appendix.**

We compare against TENT, T3A, SoTTA and ETA, four recent UDA algorithms, and also a baseline with no adaptation, (No Adapt). We do a single iteration of adaptation for all algorithms

Algorithm 2 Dynamic Entropy Control (DEC)

Input: $f_{te}, f_s, h_0, X, \kappa$

Parameters: $t_{min}, t_{max}, h_{max}, \beta, \lambda$

Output: f_s^+

```

1:  $f_s = \text{Freeze\_b\_Layers}(f_s, \beta)$ 
2:  $T_{vec} = \text{CCR}(f_{te}(X), h_0, \kappa, h_{max}, t_{min}, t_{max})$ 
   {get regularizers}
3: Initialize  $loss$ 
   {Adapt using certainty-regularized observations:}
4: for  $x_i \in X$  and  $\tau_i \in T_{vec}$  do
5:    $s_{si} = \text{SoftMax}_{T=1}(f_s(x_i))$ 
6:    $s_{ti} = \text{SoftMax}_{T=\tau_i}(f_{te}(x_i))$  {smoothen
   teacher labels}
7:    $l = (\text{avg}(T_{vec}))^2 \cdot \text{BCE}(s_{si}, s_{ti})$ 
8:   Store  $loss \leftarrow l$ 
9: end for
10:  $L = \text{avg}(loss)$ 
11:  $f'_s \leftarrow \theta_s - \lambda \nabla L(\theta_s)$ 
12:  $f_s^+ = \text{Temperature\_Scale}(f'_s, \text{avg}(T_{vec}))$ 
13: return  $f_s^+$ 

```

Algorithm	Accuracy	ECE	Entropy	Algorithm	Accuracy	ECE	Entropy
No Adapt	0.5894	0.3014	0.4386	No Adapt	0.8730	0.1054	0.0812
DEC (ours)	0.6475	0.1685	1.2195	DEC (ours)	0.8794	0.0613	0.2325
T3A	0.6247	0.2713	1.8729	T3A	0.8973	0.0844	0.0645
ETA	0.6463	0.2698	0.3561	ETA	0.8780	0.1023	0.0705
TENT	0.6445	0.2617	0.3980	TENT	0.8795	0.1007	0.0719
SoTTA	0.6399	0.2521	0.4742	SoTTA	0.8870	0.0956	0.0622

(a) Digits dataset using the SmallCNN $_{\beta=0\%}$ backbone. $\sigma_{\max}^2 = [0.22, 0.18, 0.20]$ for accuracy, ECE and entropy, respectively.

(b) PACS dataset using EfficientNet $_{\beta=98\%}$ backbone. $\sigma_{\max}^2 = [0.01, 0.02, 0.12]$ for accuracy, ECE and entropy respectively.

Table 3: Average accuracy, ECE, and entropy on Digits and PACS tested with LOO. These results show that our algorithm offers competitive accuracy uplifts while having considerably better calibration. Maximum domain-to-domain variances are reported.

unless stated otherwise. **Dataset preprocessing steps and a discussion of hyperparameters for all algorithms are in more detail in the appendix.**

4.2 Datasets

The following publicly available UDA datasets are used in our experiments; we selected these because they are commonly used in existing works and provide a variety of domain shifts. In total, **we evaluate our algorithm over 26 domain shifts**. Furthermore, 15 of our domain shifts have 5 corruption levels. For some datasets, we tested using the “leave one out” (LOO) paradigm; for example, in PACS, to test generalization to *pictures*, we first trained our backbone networks on *art*, *cartoon*, *sketch* before adapting.

1. PACS [38] has 4 domains: *pictures*, *art*, *cartoon*, *sketch* with 7 classes. Tested using LOO.
2. HomeOffice [39] has 4 domains: *art*, *clipart*, *product*, *real* with 65 classes. Tested using LOO.
3. Digits is a combination of 3 “numbers” datasets: USPS [40], MNIST [41], and SVHN [42]. There are 10 classes. Tested using LOO by training on the source domains’ training sets and adapting to target domain’s test set.
4. TinyImageNet-C (TIN-C) [43], has 15 domains with 200 classes. Backbones are trained on corruption-free (source) training set, adapted to and evaluated on corrupted (target) domains. For each target domain, there are 5 tiers of corruption.

4.3 Back Bones and Training Details

We test all but the Digits dataset on two popular low-resource classifiers, EfficientNetB0 [44] and MobileNet [45] pre-trained for ImageNet [46]. We flatten the output of both networks and add a final dense layer with an output shape equivalent to the number of classes.

We evaluate the Digits dataset using SmallCNN, a custom lightweight network tailored to handle grayscale images, serving as a representative of more compact and straightforward architectures for less complex datasets. SmallCNN encompasses a variety of essential building blocks, including 2D convolutional layers equipped with different filters, batch normalization, ReLU activation, and max-pooling layers. The network also integrates dense layers and a final classifier layer to make predictions for the given number of classes. The specific details and orderings of the layers in SmallCNN are elaborated on in the appendix. Note that all three models use batch normalization layers as necessitated by ETA, TENT, and SoTTA.

4.4 Results

We present our accuracy and ECE measurements on the four aforementioned datasets. To show evidence of the over-certainty phenomenon, we also report prediction entropy. More comprehensive figures/tables can be found in the appendix. To show the impact of our CCR algorithm, which produces our certainty regularizer τ , we perform an ablation experiment in Fig. 3.

Algorithm	Tier 1	Tier 2	Tier 3	Tier 4	Tier 5
No Adapt	0.27 _{0.04}	0.23 _{0.05}	0.19 _{0.07}	0.15 _{0.08}	0.12 _{0.08}
DEC (ours)	0.39 _{0.02}	0.37 _{0.03}	0.33 _{0.05}	0.29 _{0.07}	0.24 _{0.08}
T3A	0.27 _{0.04}	0.24 _{0.05}	0.20 _{0.07}	0.16 _{0.08}	0.13 _{0.08}
ETA	0.22 _{0.05}	0.19 _{0.06}	0.14 _{0.07}	0.11 _{0.07}	0.08 _{0.06}
TENT	0.37 _{0.03}	0.34 _{0.04}	0.30 _{0.06}	0.25 _{0.08}	0.20 _{0.09}
SoTTA	0.39 _{0.02}	0.37 _{0.03}	0.33 _{0.04}	0.29 _{0.06}	0.25 _{0.08}

Table 4: Accuracy on TIN-C with MobileNet $_{\beta=0\%}$ backbone across different tiers of corruption. Standard deviations across the domain shifts are shown as subscripts.

4.5 DEC Reduces Calibration Error

Due to our algorithm addressing the over-certainty phenomenon, we significantly improve calibration performance; DEC had the lowest average ECE in all tested datasets and in nearly all individual domain shifts. We recognize that reducing entropy *did* improve calibration compared to baseline in some cases, but the resulting calibration was still sub-optimal. Fig. 3 empirically validates our finding that an adaptive certainty regularizer aids in reducing ECE. Moreover, the variance of τ increases as the corruption intensity increases; signifying enhanced dynamic range when encountering harder observations.

We would like to underscore our algorithm’s robustness to the choice of $t_{min/max}$. **We performed our experiments by selecting our hyperparameters per dataset and NOT per domain shift.** As shown in Table 1, we achieve statistically significant reduction in ECE despite using the same hyperparameters across **15 domain shifts**. Our results in Table 2 further bolster our claims of robustness. Again, our hyperparameters are fixed across the four domain shifts but we still achieve statistically significant improvement.

4.6 DEC Augments Accuracy

In addition to strong calibration performance, DEC provides consistent accuracy uplifts while not necessitating any transformations on observations. By jointly exploiting backbone entropy and logit norm (see Fig. 2), we are able to effectively assess observation reliability. After doing so, we apply greater regularization to less reliable observations. This in turn allows us mitigate the potential label noise produced by the pseudo-labels.

Table 4 shows that our algorithm maintains competitive accuracy with recent test-time entropy minimization approaches while addressing the over-certainty phenomenon. Moreover, unlike SoTTA and T3A, **we do not store observations or training samples in any way during the adaptation process** as this could potentially cause security or privacy issues during deployment.

4.7 DEC is Suitable for Low Resource Scenarios

SmallCNN’s case in Table 3a shows our algorithm’s relevance for low-resource scenarios. We achieve strong accuracy while maintaining low calibration error. The model weights which are trainable are what predominantly consume memory for our algorithm. Therefore, the memory overhead of DEC, is controlled by β and is at most the trainable parameters of the backbone model.

In our experiments using EfficientNet, we were able to freeze the majority of the parameters of our backbone while still achieving significant performance improvements in both accuracy and ECE. Furthermore, our methodology does not require computing distance metrics between our source and target domain nor do we perform more than one backwards pass per observation. Either of which would increase computational complexity.

5 Discussion and Conclusion

Our study identifies the *over-certainty phenomenon* of state-of-the-art UDA methodologies which cause harm to model calibration. To ameliorate this issue, we introduce a certainty regularizer, τ , which persuades overall model entropy and mitigates pseudo-label noise. The resulting algorithm, DEC, jointly improves model accuracy and reduces calibration error while remaining memory efficient. Another merit of our approach is its compatibility with the majority of backbone networks.

DEC does not require batch normalization layers like SoTTA, TENT, and ETA do. This permits greater freedom when choosing a backbone. Furthermore, DEC is compatible with existing prototypical learning approaches.

References

- [1] Chuan Guo, Geoff Pleiss, Yu Sun, and Kilian Q Weinberger. On calibration of modern neural networks. In *International conference on machine learning*, pages 1321–1330. PMLR, 2017.
- [2] Moloud Abdar, Farhad Pourpanah, Sadiq Hussain, Dana Rezazadegan, Li Liu, Mohammad Ghavamzadeh, Paul Fieguth, Xiaochun Cao, Abbas Khosravi, U. Rajendra Acharya, Vladimir Makarenkov, and Saeid Nahavandi. A review of uncertainty quantification in deep learning: Techniques, applications and challenges. *Information Fusion*, 76:243–297, 2021.
- [3] Shiyu Liang, Yixuan Li, and Rayadurgam Srikant. Enhancing the reliability of out-of-distribution image detection in neural networks. *arXiv preprint arXiv:1706.02690*, 2017.
- [4] Anusri Pampari and Stefano Ermon. Unsupervised calibration under covariate shift. *arXiv preprint arXiv:2006.16405*, 2020.
- [5] Julia Grabinski, Paul Gavrikov, Janis Keuper, and Margret Keuper. Robust models are less over-confident. *Advances in Neural Information Processing Systems*, 35:39059–39075, 2022.
- [6] Yaniv Ovadia, Emily Fertig, Jie Ren, Zachary Nado, D Sculley, Sebastian Nowozin, Joshua V. Dillon, Balaji Lakshminarayanan, and Jasper Snoek. Can you trust your model’s uncertainty? evaluating predictive uncertainty under dataset shift, 2019.
- [7] Rajat Raina, Alexis Battle, Honglak Lee, Benjamin Packer, and Andrew Y Ng. Self-taught learning: transfer learning from unlabeled data. In *Proceedings of the 24th international conference on Machine learning*, pages 759–766, 2007.
- [8] Dong-Hyun Lee et al. Pseudo-label: The simple and efficient semi-supervised learning method for deep neural networks. In *Workshop on challenges in representation learning, ICML*, volume 3, page 896. Atlanta, 2013.
- [9] Massimiliano Mancini, Samuel Rota Buló, Barbara Caputo, and Elisa Ricci. Best sources forward: domain generalization through source-specific nets. In *2018 25th IEEE international conference on image processing (ICIP)*, pages 1353–1357. IEEE, 2018.
- [10] Jindong Wang, Cuiling Lan, Chang Liu, Yidong Ouyang, Tao Qin, Wang Lu, Yiqiang Chen, Wenjun Zeng, and Philip Yu. Generalizing to unseen domains: A survey on domain generalization. *IEEE Transactions on Knowledge and Data Engineering*, 2022.
- [11] Geoffrey Hinton, Oriol Vinyals, and Jeffrey Dean. Distilling the knowledge in a neural network. In *NIPS Deep Learning and Representation Learning Workshop*, 2015.
- [12] Jianping Gou, Baosheng Yu, Stephen J Maybank, and Dacheng Tao. Knowledge distillation: A survey. *International Journal of Computer Vision*, 129:1789–1819, 2021.
- [13] Samuel Stanton, Pavel Izmailov, Polina Kirichenko, Alexander A Alemi, and Andrew G Wilson. Does knowledge distillation really work? *Advances in Neural Information Processing Systems*, 34:6906–6919, 2021.
- [14] Dequan Wang, Evan Shelhamer, Shaoteng Liu, Bruno Olshausen, and Trevor Darrell. Tent: Fully test-time adaptation by entropy minimization. *arXiv preprint arXiv:2006.10726*, 2020.
- [15] Shuaicheng Niu, Jiayang Wu, Yifan Zhang, Yaofu Chen, Shijian Zheng, Peilin Zhao, and Mingkui Tan. Efficient test-time model adaptation without forgetting. In *International conference on machine learning*, pages 16888–16905. PMLR, 2022.
- [16] Yusuke Iwasawa and Yutaka Matsuo. Test-time classifier adjustment module for model-agnostic domain generalization. *Advances in Neural Information Processing Systems*, 34:2427–2440, 2021.
- [17] Taesik Gong, Yewon Kim, Taekyung Lee, Sorn Chottananurak, and Sung-Ju Lee. Sotta: Robust test-time adaptation on noisy data streams. *Advances in Neural Information Processing Systems*, 36, 2024.
- [18] Pierre Foret, Ariel Kleiner, Hossein Mobahi, and Behnam Neyshabur. Sharpness-aware minimization for efficiently improving generalization. *arXiv preprint arXiv:2010.01412*, 2020.

- [19] Jake Snell, Kevin Swersky, and Richard Zemel. Prototypical networks for few-shot learning. *Advances in neural information processing systems*, 30, 2017.
- [20] Surat Teerapittayanon, Bradley McDanel, and H. T. Kung. Branchynet: Fast inference via early exiting from deep neural networks. *CoRR*, abs/1709.01686, 2017.
- [21] Weicheng Zhu, Matan Leibovich, Sheng Liu, Sreyas Mohan, Aakash Kaku, Boyang Yu, Laure Zanna, Narges Razavian, and Carlos Fernandez-Granda. Deep probability estimation, 2022.
- [22] Hongxin Wei, Renchunzi Xie, Hao Cheng, Lei Feng, Bo An, and Yixuan Li. Mitigating neural network overconfidence with logit normalization. In *International Conference on Machine Learning*, pages 23631–23644. PMLR, 2022.
- [23] Chang-Bin Zhang, Peng-Tao Jiang, Qibin Hou, Yunchao Wei, Qi Han, Zhen Li, and Ming-Ming Cheng. Delving deep into label smoothing. *IEEE Transactions on Image Processing*, 30:5984–5996, 2021.
- [24] Rafael Müller, Simon Kornblith, and Geoffrey E. Hinton. When does label smoothing help? *CoRR*, abs/1906.02629, 2019.
- [25] Kai Tian, Shuigeng Zhou, Jianping Fan, and Jihong Guan. Learning competitive and discriminative reconstructions for anomaly detection. In *Proceedings of the AAAI Conference on Artificial Intelligence*, volume 33, pages 5167–5174, 2019.
- [26] Thomas Schlegl, Philipp Seeböck, Sebastian M. Waldstein, Ursula Schmidt-Erfurth, and Georg Langs. Unsupervised anomaly detection with generative adversarial networks to guide marker discovery. *CoRR*, abs/1703.05921, 2017.
- [27] Houssam Zenati, Chuan Sheng Foo, Bruno Lecouat, Gaurav Manek, and Vijay Ramaseshan Chandrasekhar. Efficient gan-based anomaly detection, 2018.
- [28] Abhijit Bendale and Terrance E Boult. Towards open set deep networks. In *Proceedings of the IEEE conference on computer vision and pattern recognition*, pages 1563–1572, 2016.
- [29] Yifei Ming, Ziyang Cai, Jiuxiang Gu, Yiyun Sun, Wei Li, and Yixuan Li. Delving into out-of-distribution detection with vision-language representations. *Advances in Neural Information Processing Systems*, 35:35087–35102, 2022.
- [30] Jaewoo Park, Jacky Chen Long Chai, Jaeho Yoon, and Andrew Beng Jin Teoh. Understanding the feature norm for out-of-distribution detection. In *Proceedings of the IEEE/CVF International Conference on Computer Vision*, pages 1557–1567, 2023.
- [31] Xue Jiang, Feng Liu, Zhen Fang, Hong Chen, Tongliang Liu, Feng Zheng, and Bo Han. Detecting out-of-distribution data through in-distribution class prior. In *International Conference on Machine Learning*, pages 15067–15088. PMLR, 2023.
- [32] Xinheng Wu, Jie Lu, Zhen Fang, and Guangquan Zhang. Meta ood learning for continuously adaptive ood detection. In *Proceedings of the IEEE/CVF International Conference on Computer Vision*, pages 19353–19364, 2023.
- [33] Wenjun Miao, Guansong Pang, Tianqi Li, Xiao Bai, and Jin Zheng. Out-of-distribution detection in long-tailed recognition with calibrated outlier class learning. *arXiv preprint arXiv:2312.10686*, 2023.
- [34] Zhen Fang, Yixuan Li, Jie Lu, Jiahua Dong, Bo Han, and Feng Liu. Is out-of-distribution detection learnable? *Advances in Neural Information Processing Systems*, 35:37199–37213, 2022.
- [35] Qizhe Xie, Minh-Thang Luong, Eduard Hovy, and Quoc V Le. Self-training with noisy student improves imagenet classification. In *Proceedings of the IEEE/CVF conference on computer vision and pattern recognition*, pages 10687–10698, 2020.
- [36] Michal Lukasik, Srinadh Bhojanapalli, Aditya Menon, and Sanjiv Kumar. Does label smoothing mitigate label noise? In Hal Daumé III and Aarti Singh, editors, *Proceedings of the 37th International Conference on Machine Learning*, volume 119 of *Proceedings of Machine Learning Research*, pages 6448–6458. PMLR, 13–18 Jul 2020.
- [37] Ori Press, Ravid Shwartz-Ziv, Yann LeCun, and Matthias Bethge. The entropy enigma: Success and failure of entropy minimization. *arXiv preprint arXiv:2405.05012*, 2024.

- [38] Da Li, Yongxin Yang, Yi-Zhe Song, and Timothy M Hospedales. Deeper, broader and artier domain generalization. In *Proceedings of the IEEE international conference on computer vision*, pages 5542–5550, 2017.
- [39] Hemanth Venkateswara, Jose Eusebio, Shayok Chakraborty, and Sethuraman Panchanathan. Deep hashing network for unsupervised domain adaptation. In *Proceedings of the IEEE conference on computer vision and pattern recognition*, pages 5018–5027, 2017.
- [40] J.J. Hull. A database for handwritten text recognition research. *IEEE Transactions on Pattern Analysis and Machine Intelligence*, 16(5):550–554, 1994.
- [41] Yann LeCun, Corinna Cortes, and CJ Burges. Mnist handwritten digit database. *ATT Labs [Online]*. Available: <http://yann.lecun.com/exdb/mnist>, 2, 2010.
- [42] Yuval Netzer, Tao Wang, Adam Coates, Alessandro Bissacco, Bo Wu, and Andrew Y Ng. Reading digits in natural images with unsupervised feature learning. *Neurips Workshop on Deep Learning*, 2011.
- [43] Ya Le and Xuan Yang. Tiny imagenet visual recognition challenge. *CS 231N*, 7(7):3, 2015.
- [44] Mingxing Tan and Quoc V. Le. Efficientnet: Rethinking model scaling for convolutional neural networks. *CoRR*, abs/1905.11946, 2019.
- [45] Andrew G. Howard, Menglong Zhu, Bo Chen, Dmitry Kalenichenko, Weijun Wang, Tobias Weyand, Marco Andreetto, and Hartwig Adam. Mobilenets: Efficient convolutional neural networks for mobile vision applications, 2017.
- [46] Jia Deng, Wei Dong, Richard Socher, Li-Jia Li, Kai Li, and Li Fei-Fei. Imagenet: A large-scale hierarchical image database. In *2009 IEEE conference on computer vision and pattern recognition*, pages 248–255. Ieee, 2009.